

Limits on the production of narrow $t\bar{t}$ resonances in $p\bar{p}$ collisions at $\sqrt{s} = 1.96$ TeV

T. Aaltonen,²³ J. Adelman,¹³ T. Akimoto,⁵⁴ M. G. Albrow,¹⁷ B. Álvarez González,¹¹ S. Amerio,⁴² D. Amidei,³⁴ A. Anastassov,⁵¹ A. Annovi,¹⁹ J. Antos,¹⁴ M. Aoki,²⁴ G. Apollinari,¹⁷ A. Apresyan,⁴⁷ T. Arisawa,⁵⁶ A. Artikov,¹⁵ W. Ashmanskas,¹⁷ A. Attal,³ A. Aurisano,⁵² F. Azfar,⁴¹ P. Azzi-Bacchetta,⁴² P. Azzurri,⁴⁵ N. Bacchetta,⁴² W. Badgett,¹⁷ A. Barbaro-Galtieri,²⁸ V. E. Barnes,⁴⁷ B. A. Barnett,²⁵ S. Baroiant,⁷ V. Bartsch,³⁰ G. Bauer,³² P.-H. Beauchemin,³³ F. Bedeschi,⁴⁵ P. Bednar,¹⁴ S. Behari,²⁵ G. Bellettini,⁴⁵ J. Bellinger,⁵⁸ A. Belloni,²² D. Benjamin,¹⁶ A. Beretvas,¹⁷ J. Beringer,²⁸ T. Berry,²⁹ A. Bhatti,⁴⁹ M. Binkley,¹⁷ D. Bisello,⁴² I. Bizjak,³⁰ R. E. Blair,² C. Blocker,⁶ B. Blumenfeld,²⁵ A. Bocci,¹⁶ A. Bodek,⁴⁸ V. Boisvert,⁴⁸ G. Bolla,⁴⁷ A. Bolshov,³² D. Bortoletto,⁴⁷ J. Boudreau,⁴⁶ A. Boveia,¹⁰ B. Brau,¹⁰ A. Bridgeman,²⁴ L. Brigliadori,⁵ C. Bromberg,³⁵ E. Brubaker,¹³ J. Budagov,¹⁵ H. S. Budd,⁴⁸ S. Budd,²⁴ K. Burkett,¹⁷ G. Busetto,⁴² P. Bussey,²¹ A. Buzatu,³³ K. L. Byrum,² S. Cabrera,^{16,s} M. Campanelli,³⁵ M. Campbell,³⁴ F. Canelli,¹⁷ A. Canepa,⁴⁴ D. Carlsmith,⁵⁸ R. Carosi,⁴⁵ S. Carrillo,^{18,m} S. Carron,³³ B. Casal,¹¹ M. Casarsa,¹⁷ A. Castro,⁵ P. Catastini,⁴⁵ D. Cauz,⁵³ M. Cavalli-Sforza,³ A. Cerri,²⁸ L. Cerrito,^{30,q} S. H. Chang,²⁷ Y. C. Chen,¹ M. Chertok,⁷ G. Chiarelli,⁴⁵ G. Chlachidze,¹⁷ F. Chlebana,¹⁷ K. Cho,²⁷ D. Chokheli,¹⁵ J. P. Chou,²² G. Choudalakis,³² S. H. Chuang,⁵¹ K. Chung,¹² W. H. Chung,⁵⁸ Y. S. Chung,⁴⁸ C. I. Ciobanu,²⁴ M. A. Ciocci,⁴⁵ A. Clark,²⁰ D. Clark,⁶ G. Compostella,⁴² M. E. Convery,¹⁷ J. Conway,⁷ B. Cooper,³⁰ K. Copic,³⁴ M. Cordelli,¹⁹ G. Cortiana,⁴² F. Crescioli,⁴⁵ C. Cuenca Almenar,^{7,s} J. Cuevas,^{11,p} R. Culbertson,¹⁷ J. C. Cully,³⁴ D. Dagenhart,¹⁷ M. Datta,¹⁷ T. Davies,²¹ P. de Barbaro,⁴⁸ S. De Cecco,⁵⁰ A. Deisher,²⁸ G. De Lentdecker,^{48,e} G. De Lorenzo,³ M. Dell'Orso,⁴⁵ L. Demortier,⁴⁹ J. Deng,¹⁶ M. Deninno,⁵ D. De Pedis,⁵⁰ P. F. Derwent,¹⁷ G. P. Di Giovanni,⁴³ C. Dionisi,⁵⁰ B. Di Ruzza,⁵³ J. R. Dittmann,⁴ M. D'Onofrio,³ S. Donati,⁴⁵ P. Dong,⁸ J. Donini,⁴² T. Dorigo,⁴² S. Dube,⁵¹ J. Efron,³⁸ R. Erbacher,⁷ D. Errede,²⁴ S. Errede,²⁴ R. Eusebi,¹⁷ H. C. Fang,²⁸ S. Farrington,²⁹ W. T. Fedorko,¹³ R. G. Feild,⁵⁹ M. Feindt,²⁶ J. P. Fernandez,³¹ C. Ferrazza,⁴⁵ R. Field,¹⁸ G. Flanagan,⁴⁷ R. Forrest,⁷ S. Forrester,⁷ M. Franklin,²² J. C. Freeman,²⁸ I. Furic,¹⁸ M. Gallinaro,⁴⁹ J. Galyardt,¹² F. Garbersson,¹⁰ J. E. Garcia,⁴⁵ A. F. Garfinkel,⁴⁷ H. Gerberich,²⁴ D. Gerdes,³⁴ S. Giagu,⁵⁰ V. Giakoumopolou,^{45,b} P. Giannetti,⁴⁵ K. Gibson,⁴⁶ J. L. Gimmell,⁴⁸ C. M. Ginsburg,¹⁷ N. Giokaris,^{15,b} M. Giordani,⁵³ P. Giromini,¹⁹ M. Giunta,⁴⁵ V. Glagolev,¹⁵ D. Glenzinski,¹⁷ M. Gold,³⁶ N. Goldschmidt,¹⁸ A. Golossanov,¹⁷ G. Gomez,¹¹ G. Gomez-Ceballos,³² M. Goncharov,⁵² O. González,³¹ I. Gorelov,³⁶ A. T. Goshaw,¹⁶ K. Goulianos,⁴⁹ A. Gresele,⁴² S. Grinstein,²² C. Grosso-Pilcher,¹³ R. C. Group,¹⁷ U. Grundler,²⁴ J. Guimaraes da Costa,²² Z. Gunay-Unalan,³⁵ C. Haber,²⁸ K. Hahn,³² S. R. Hahn,¹⁷ E. Halkiadakis,⁵¹ A. Hamilton,²⁰ B.-Y. Han,⁴⁸ J. Y. Han,⁴⁸ R. Handler,⁵⁸ F. Happacher,¹⁹ K. Hara,⁵⁴ D. Hare,⁵¹ M. Hare,⁵⁵ S. Harper,⁴¹ R. F. Harr,⁵⁷ R. M. Harris,¹⁷ M. Hartz,⁴⁶ K. Hatakeyama,⁴⁹ J. Hauser,⁸ C. Hays,⁴¹ M. Heck,²⁶ A. Heijboer,⁴⁴ B. Heinemann,²⁸ J. Heinrich,⁴⁴ C. Henderson,³² M. Herndon,⁵⁸ J. Heuser,²⁶ S. Hewamanage,⁴ D. Hidas,¹⁶ C. S. Hill,^{10,d} D. Hirschbuehl,²⁶ A. Hocker,¹⁷ S. Hou,¹ M. Houlden,²⁹ S.-C. Hsu,⁹ B. T. Huffman,⁴¹ R. E. Hughes,³⁸ U. Husemann,⁵⁹ J. Huston,³⁵ J. Incandela,¹⁰ G. Introzzi,⁴⁵ M. Iori,⁵⁰ A. Ivanov,⁷ B. Iyutin,³² E. James,¹⁷ B. Jayatilaka,¹⁶ D. Jeans,⁵⁰ E. J. Jeon,²⁷ S. Jindariani,¹⁸ W. Johnson,⁷ M. Jones,⁴⁷ K. K. Joo,²⁷ S. Y. Jun,¹² J. E. Jung,²⁷ T. R. Junk,²⁴ M. Kagan,³⁴ T. Kamon,⁵² D. Kar,¹⁸ P. E. Karchin,⁵⁷ Y. Kato,⁴⁰ R. Kephart,¹⁷ U. Kerzel,²⁶ V. Khotilovich,⁵² B. Kilminster,³⁸ D. H. Kim,²⁷ H. S. Kim,²⁷ J. E. Kim,²⁷ M. J. Kim,¹⁷ S. B. Kim,²⁷ S. H. Kim,⁵⁴ Y. K. Kim,¹³ N. Kimura,⁵⁴ L. Kirsch,⁶ S. Klimenko,¹⁸ M. Klute,³² B. Knuteson,³² B. R. Ko,¹⁶ S. A. Koay,¹⁰ K. Kondo,⁵⁶ D. J. Kong,²⁷ J. Konigsberg,¹⁸ A. Korytov,¹⁸ A. V. Kotwal,¹⁶ J. Kraus,²⁴ M. Kreps,²⁶ J. Kroll,⁴⁴ N. Krumnack,⁴ M. Kruse,¹⁶ V. Krutelyov,¹⁰ T. Kubo,⁵⁴ S. E. Kuhlmann,² T. Kuhr,²⁶ N. P. Kulkarni,⁵⁷ Y. Kusakabe,⁵⁶ S. Kwang,¹³ A. T. Laasanen,⁴⁷ S. Lai,³³ S. Lami,⁴⁵ S. Lammel,¹⁷ M. Lancaster,³⁰ R. L. Lander,⁷ K. Lannon,³⁸ A. Lath,⁵¹ G. Latino,⁴⁵ I. Lazzizzera,⁴² T. LeCompte,² J. Lee,⁴⁸ J. Lee,²⁷ Y. J. Lee,²⁷ S. W. Lee,^{52,r} R. Lefèvre,²⁰ N. Leonardo,³² S. Leone,⁴⁵ S. Levy,¹³ J. D. Lewis,¹⁷ C. Lin,⁵⁹ C. S. Lin,²⁸ J. Linacre,⁴¹ M. Lindgren,¹⁷ E. Lipeles,⁹ A. Lister,⁷ D. O. Litvintsev,¹⁷ T. Liu,¹⁷ N. S. Lockyer,⁴⁴ A. Loginov,⁵⁹ M. Loretì,⁴² L. Lovas,¹⁴ R.-S. Lu,¹ D. Lucchesi,⁴² J. Lueck,²⁶ C. Luci,⁵⁰ P. Lujan,²⁸ P. Lukens,¹⁷ G. Lungu,¹⁸ L. Lyons,⁴¹ J. Lys,²⁸ R. Lysak,¹⁴ E. Lytken,⁴⁷ P. Mack,²⁶ D. MacQueen,³³ R. Madrak,¹⁷ K. Maeshima,¹⁷ K. Makhoul,³² T. Maki,²³ P. Maksimovic,²⁵ S. Malde,⁴¹ S. Malik,³⁰ G. Manca,²⁹ A. Manousakis,^{15,b} F. Margaroli,⁴⁷ C. Marino,²⁶ C. P. Marino,²⁴ A. Martin,⁵⁹ M. Martin,²⁵ V. Martin,^{21,k} M. Martínez,³ R. Martínez-Ballarín,³¹ T. Maruyama,⁵⁴ P. Mastrandrea,⁵⁰ T. Masubuchi,⁵⁴ M. E. Mattson,⁵⁷ P. Mazzanti,⁵ K. S. McFarland,⁴⁸ P. McIntyre,⁵² R. McNulty,^{29,j} A. Mehta,²⁹ P. Mehtala,²³ S. Menzemer,^{11,l} A. Menzione,⁴⁵ P. Merkel,⁴⁷ C. Mesropian,⁴⁹ A. Messina,³⁵ T. Miao,¹⁷ N. Miladinovic,⁶ J. Miles,³² R. Miller,³⁵ C. Mills,²² M. Milnik,²⁶ A. Mitra,¹ G. Mitselmakher,¹⁸ H. Miyake,⁵⁴ S. Moed,²² N. Moggi,⁵ C. S. Moon,²⁷ R. Moore,¹⁷ M. Morello,⁴⁵ P. Movilla Fernandez,²⁸ J. Mülmenstädt,²⁸ A. Mukherjee,¹⁷ Th. Müller,²⁶ R. Mumford,²⁵ P. Murat,¹⁷ M. Mussini,⁵ J. Nachtman,¹⁷ Y. Nagai,⁵⁴ A. Nagano,⁵⁴ J. Naganoma,⁵⁶ K. Nakamura,⁵⁴ I. Nakano,³⁹ A. Napier,⁵⁵ V. Necula,¹⁶ C. Neu,⁴⁴ M. S. Neubauer,²⁴ J. Nielsen,^{28,g} L. Nodulman,² M. Norman,⁹

O. Norriella,²⁴ E. Nurse,³⁰ S. H. Oh,¹⁶ Y. D. Oh,²⁷ I. Oksuzian,¹⁸ T. Okusawa,⁴⁰ R. Oldeman,²⁹ R. Orava,²³ K. Osterberg,²³ S. Pagan Griso,⁴² C. Pagliarone,⁴⁵ E. Palencia,¹⁷ V. Papadimitriou,¹⁷ A. Papaikonomou,²⁶ A. A. Paramonov,¹³ B. Parks,³⁸ S. Pashapour,³³ J. Patrick,¹⁷ G. Pauletta,⁵³ M. Paulini,¹² C. Paus,³² D. E. Pellett,⁷ A. Penzo,⁵³ T. J. Phillips,¹⁶ G. Piacentino,⁴⁵ J. Piedra,⁴³ L. Pina,¹⁸ K. Pitts,²⁴ C. Plager,⁸ L. Pondrom,⁵⁸ X. Portell,³ O. Poukhov,¹⁵ N. Pounder,⁴¹ F. Prakoshyn,⁴⁵ A. Pronko,¹⁷ J. Proudfoot,² F. Ptohos,^{17,i} G. Punzi,⁴⁵ J. Pursley,⁵⁸ J. Rademacker,^{41,d} A. Rahaman,⁴⁶ V. Ramakrishnan,⁵⁸ N. Ranjan,⁴⁷ I. Redondo,³¹ B. Reisert,¹⁷ V. Rekovic,³⁶ P. Renton,⁴¹ M. Rescigno,⁵⁰ S. Richter,²⁶ F. Rimondi,⁵ L. Ristori,⁴⁵ A. Robson,²¹ T. Rodrigo,¹¹ E. Rogers,²⁴ S. Rolli,⁵⁵ R. Roser,¹⁷ M. Rossi,⁵³ R. Rossin,¹⁰ P. Roy,³³ A. Ruiz,¹¹ J. Russ,¹² V. Rusu,¹⁷ H. Saarikko,²³ A. Safonov,⁵² W. K. Sakumoto,⁴⁸ G. Salamanna,⁵⁰ O. Saltó,³ L. Santi,⁵³ S. Sarkar,⁵⁰ L. Sartori,⁴⁵ K. Sato,¹⁷ P. Savard,³³ A. Savoy-Navarro,⁴³ T. Scheidle,²⁶ P. Schlabach,¹⁷ E. E. Schmidt,¹⁷ M. A. Schmidt,¹³ M. P. Schmidt,⁵⁹ M. Schmitt,³⁷ T. Schwarz,⁷ L. Scodellaro,¹¹ A. L. Scott,¹⁰ A. Scribano,⁴⁵ F. Scuri,⁴⁵ A. Sedov,⁴⁷ S. Seidel,³⁶ Y. Seiya,⁴⁰ A. Semenov,¹⁵ L. Sexton-Kennedy,¹⁷ A. Sfyria,²⁰ S. Z. Shalhout,⁵⁷ M. D. Shapiro,²⁸ T. Shears,²⁹ P. F. Shepard,⁴⁶ D. Sherman,²² M. Shimojima,^{54,o} M. Shochet,¹³ Y. Shon,⁵⁸ I. Shreyber,²⁰ A. Sidoti,⁴⁵ P. Sinervo,³³ A. Sisakyan,¹⁵ A. J. Slaughter,¹⁷ J. Slaunwhite,³⁸ K. Sliwa,⁵⁵ J. R. Smith,⁷ F. D. Snider,¹⁷ R. Snihur,³³ M. Soderberg,³⁴ A. Soha,⁷ S. Somalwar,⁵¹ V. Sorin,³⁵ J. Spalding,¹⁷ F. Spinella,⁴⁵ T. Spreitzer,³³ P. Squillacioti,⁴⁵ M. Stanitzki,⁵⁹ R. St. Denis,²¹ B. Stelzer,⁸ O. Stelzer-Chilton,⁴¹ D. Stentz,³⁷ J. Strologas,³⁶ D. Stuart,¹⁰ J. S. Suh,²⁷ A. Sukhanov,¹⁸ H. Sun,⁵⁵ I. Suslov,¹⁵ T. Suzuki,⁵⁴ A. Taffard,^{24,f} R. Takashima,³⁹ Y. Takeuchi,⁵⁴ R. Tanaka,³⁹ M. Tecchio,³⁴ P. K. Teng,¹ K. Terashi,⁴⁹ J. Thom,^{17,h} A. S. Thompson,²¹ G. A. Thompson,²⁴ E. Thomson,⁴⁴ P. Tipton,⁵⁹ V. Tiwari,¹² S. Tkaczyk,¹⁷ D. Toback,⁵² S. Tokar,¹⁴ K. Tollefson,³⁵ T. Tomura,⁵⁴ D. Tonelli,¹⁷ S. Torre,¹⁹ D. Torretta,¹⁷ S. Tournear,⁴³ W. Trischuk,³³ Y. Tu,⁴⁴ N. Turini,⁴⁵ F. Ukegawa,⁵⁴ S. Uozumi,⁵⁴ S. Vallecorsa,²⁰ N. van Remortel,²³ A. Varganov,³⁴ E. Vataha,³⁶ F. Vázquez,^{18,m} G. Velev,¹⁷ C. Vellidis,^{45,b} V. Veszpremi,⁴⁷ M. Vidal,³¹ R. Vidal,¹⁷ I. Vila,¹¹ R. Vilar,¹¹ T. Vine,³⁰ M. Vogel,³⁶ I. Volobouev,^{28,r} G. Volpi,⁴⁵ F. Würthwein,⁹ P. Wagner,⁴⁴ R. G. Wagner,² R. L. Wagner,¹⁷ J. Wagner,²⁶ W. Wagner,²⁶ T. Wakisaka,⁴⁰ R. Wallny,⁸ S. M. Wang,¹ A. Warburton,³³ D. Waters,³⁰ M. Weinberger,⁵² W. C. Wester III,¹⁷ B. Whitehouse,⁵⁵ D. Whiteson,^{44,f} A. B. Wicklund,² E. Wicklund,¹⁷ G. Williams,³³ H. H. Williams,⁴⁴ P. Wilson,¹⁷ B. L. Winer,³⁸ P. Wittich,^{17,h} S. Wolbers,¹⁷ C. Wolfe,¹³ T. Wright,³⁴ X. Wu,²⁰ S. M. Wynne,²⁹ A. Yagil,⁹ K. Yamamoto,⁴⁰ J. Yamaoka,⁵¹ T. Yamashita,³⁹ C. Yang,⁵⁹ U. K. Yang,^{13,n} Y. C. Yang,²⁷ W. M. Yao,²⁸ G. P. Yeh,¹⁷ J. Yoh,¹⁷ K. Yorita,¹³ T. Yoshida,⁴⁰ G. B. Yu,⁴⁸ I. Yu,²⁷ S. S. Yu,¹⁷ J. C. Yun,¹⁷ L. Zanello,⁵⁰ A. Zanetti,⁵³ I. Zaw,²² X. Zhang,²⁴ Y. Zheng,^{8,c} and S. Zucchelli⁵

(CDF Collaboration)^a¹*Institute of Physics, Academia Sinica, Taipei, Taiwan 11529, Republic of China*²*Argonne National Laboratory, Argonne, Illinois 60439, USA*³*Institut de Física d'Altes Energies, Universitat Autònoma de Barcelona, E-08193, Bellaterra (Barcelona), Spain*⁴*Baylor University, Waco, Texas 76798, USA*⁵*Istituto Nazionale di Fisica Nucleare, University of Bologna, I-40127 Bologna, Italy*⁶*Brandeis University, Waltham, Massachusetts 02254, USA*⁷*University of California, Davis, Davis, California 95616, USA*⁸*University of California, Los Angeles, Los Angeles, California 90024, USA*⁹*University of California, San Diego, La Jolla, California 92093, USA*¹⁰*University of California, Santa Barbara, Santa Barbara, California 93106, USA*¹¹*Instituto de Física de Cantabria, CSIC-University of Cantabria, 39005 Santander, Spain*¹²*Carnegie Mellon University, Pittsburgh, Pennsylvania 15213, USA*¹³*Enrico Fermi Institute, University of Chicago, Chicago, Illinois 60637, USA*¹⁴*Comenius University, 842 48 Bratislava, Slovakia**and Institute of Experimental Physics, 040 01 Kosice, Slovakia*¹⁵*Joint Institute for Nuclear Research, RU-141980 Dubna, Russia*¹⁶*Duke University, Durham, North Carolina 27708*¹⁷*Fermi National Accelerator Laboratory, Batavia, Illinois 60510, USA*¹⁸*University of Florida, Gainesville, Florida 32611, USA*¹⁹*Laboratori Nazionali di Frascati, Istituto Nazionale di Fisica Nucleare, I-00044 Frascati, Italy*²⁰*University of Geneva, CH-1211 Geneva 4, Switzerland*²¹*Glasgow University, Glasgow G12 8QQ, United Kingdom*²²*Harvard University, Cambridge, Massachusetts 02138, USA*²³*Division of High Energy Physics, Department of Physics, University of Helsinki and Helsinki Institute of Physics, FIN-00014, Helsinki, Finland*

- ²⁴University of Illinois, Urbana, Illinois 61801, USA
- ²⁵The Johns Hopkins University, Baltimore, Maryland 21218, USA
- ²⁶Institut für Experimentelle Kernphysik, Universität Karlsruhe, 76128 Karlsruhe, Germany
- ²⁷Center for High Energy Physics: Kyungpook National University, Daegu 702-701, Korea and Seoul National University, Seoul 151-742, Korea and Sungkyunkwan University, Suwon 440-746, Korea and Korea Institute of Science and Technology Information, Daejeon, 305-806, Korea and Chonnam National University, Gwangju, 500-757, Korea
- ²⁸Ernest Orlando Lawrence Berkeley National Laboratory, Berkeley, California 94720, USA
- ²⁹University of Liverpool, Liverpool L69 7ZE, United Kingdom
- ³⁰University College London, London WC1E 6BT, United Kingdom
- ³¹Centro de Investigaciones Energeticas Medioambientales y Tecnologicas, E-28040 Madrid, Spain
- ³²Massachusetts Institute of Technology, Cambridge, Massachusetts 02139, USA
- ³³Institute of Particle Physics: McGill University, Montréal, Canada H3A 2T8; and University of Toronto, Toronto, Canada M5S 1A7
- ³⁴University of Michigan, Ann Arbor, Michigan 48109, USA
- ³⁵Michigan State University, East Lansing, Michigan 48824, USA
- ³⁶University of New Mexico, Albuquerque, New Mexico 87131, USA
- ³⁷Northwestern University, Evanston, Illinois 60208, USA
- ³⁸The Ohio State University, Columbus, Ohio 43210, USA
- ³⁹Okayama University, Okayama 700-8530, Japan
- ⁴⁰Osaka City University, Osaka 588, Japan
- ⁴¹University of Oxford, Oxford OX1 3RH, United Kingdom
- ⁴²University of Padova, Istituto Nazionale di Fisica Nucleare, Sezione di Padova-Trento, I-35131 Padova, Italy
- ⁴³LPNHE, Universite Pierre et Marie Curie/IN2P3-CNRS, UMR7585, Paris, F-75252 France
- ⁴⁴University of Pennsylvania, Philadelphia, Pennsylvania 19104, USA
- ⁴⁵Istituto Nazionale di Fisica Nucleare Pisa, Universities of Pisa, Siena and Scuola Normale Superiore, I-56127 Pisa, Italy
- ⁴⁶University of Pittsburgh, Pittsburgh, Pennsylvania 15260, USA
- ⁴⁷Purdue University, West Lafayette, Indiana 47907, USA
- ⁴⁸University of Rochester, Rochester, New York 14627, USA
- ⁴⁹The Rockefeller University, New York, New York 10021, USA
- ⁵⁰Istituto Nazionale di Fisica Nucleare, Sezione di Roma 1, University of Rome "La Sapienza," I-00185 Roma, Italy
- ⁵¹Rutgers University, Piscataway, New Jersey 08855, USA
- ⁵²Texas A&M University, College Station, Texas 77843, USA
- ⁵³Istituto Nazionale di Fisica Nucleare, University of Trieste/ Udine, Italy
- ⁵⁴University of Tsukuba, Tsukuba, Ibaraki 305, Japan
- ⁵⁵Tufts University, Medford, Massachusetts 02155, USA
- ⁵⁶Waseda University, Tokyo 169, Japan
- ⁵⁷Wayne State University, Detroit, Michigan 48201, USA

^aURL: <http://www-cdf.fnal.gov>

^bUniversity of Athens, 15784 Athens, Greece.

^cVisiting from: Chinese Academy of Sciences, Beijing 100864, China.

^dVisiting from: University of Bristol, Bristol BS8 1TL, United Kingdom.

^eVisiting from: University Libre de Bruxelles, B-1050 Brussels, Belgium.

^fVisiting from: University of California Irvine, Irvine, CA 92697, USA.

^gVisiting from: University of California Santa Cruz, Santa Cruz, CA 95064, USA.

^hVisiting from: Cornell University, Ithaca, NY 14853, USA.

ⁱVisiting from: University of Cyprus, Nicosia CY-1678, Cyprus.

^jVisiting from: University College Dublin, Dublin 4, Ireland.

^kVisiting from: University of Edinburgh, Edinburgh EH9 3JZ, United Kingdom.

^lVisiting from: University of Heidelberg, D-69120 Heidelberg, Germany.

^mVisiting from: Universidad Iberoamericana, Mexico D.F., Mexico.

ⁿVisiting from: University of Manchester, Manchester M13 9PL, England.

^oVisiting from: Nagasaki Institute of Applied Science, Nagasaki, Japan.

^pVisiting from: University de Oviedo, E-33007 Oviedo, Spain.

^qVisiting from: Queen Mary, University of London, London, E1 4NS, England.

^rVisiting from: Texas Tech University, Lubbock, TX 79409, USA.

^sVisiting from: IFIC(CSIC-Universitat de Valencia), 46071 Valencia, Spain.

⁵⁸*University of Wisconsin, Madison, Wisconsin 53706, USA*⁵⁹*Yale University, New Haven, Connecticut 06520, USA*

(Received 30 October 2007; published 12 March 2008)

We search for evidence of resonant top quark pair production in 955 pb^{-1} of $p\bar{p}$ collisions at $\sqrt{s} = 1.96 \text{ TeV}$ recorded with the CDF II detector at the Fermilab Tevatron. For fully reconstructed candidate $t\bar{t}$ events triggered on leptons with large transverse momentum and containing at least one identified b -quark jet, we compare the invariant mass spectrum of $t\bar{t}$ pairs to the expected superposition of standard model $t\bar{t}$, non- $t\bar{t}$ backgrounds, and a simple resonance model based on a sequential Z' boson. We establish upper limits for $\sigma(p\bar{p} \rightarrow Z') \cdot Br(Z' \rightarrow t\bar{t})$ in the Z' mass interval from $450 \text{ GeV}/c^2$ to $900 \text{ GeV}/c^2$. A topcolor leptophobic Z' is ruled out below $720 \text{ GeV}/c^2$, and the cross section of any narrow Z' -like state decaying to $t\bar{t}$ is found to be less than 0.64 pb at 95% C.L. for $M_{Z'}$ above $700 \text{ GeV}/c^2$.

DOI: [10.1103/PhysRevD.77.051102](https://doi.org/10.1103/PhysRevD.77.051102)

PACS numbers: 13.85.Rm, 14.65.Ha, 14.80.-j

Resonant top pair production in hadronic collisions has been discussed in the context of extended gauge theories with massive Z -like bosons [1–3], in theories with topcolor [4], or with axigluons [5]. Decays to $t\bar{t}$ are of special interest in leptophobic models that would evade detection in traditional searches based on dielectron or dimuon signatures. More recently, resonant top pairs have been suggested as signatures for Kaluza-Klein (KK) states of gluons, weak bosons, and gravitons [6–8]; in some of these models the KK excitation couples strongly to the top quark and $t\bar{t}$ is the dominant decay mode.

A $t\bar{t}$ resonance would appear as unexpected structure in the spectrum of the invariant mass of $t\bar{t}$ pairs $M_{t\bar{t}}$. Previous searches using $\approx 100 \text{ pb}^{-1}$ samples from Fermilab Tevatron Run I have ruled out the production of a narrow leptophobic topcolor resonance with mass less than $480 \text{ GeV}/c^2$ [9,10]. Here, we search for resonant structure in the $M_{t\bar{t}}$ spectrum in 955 pb^{-1} of $p\bar{p}$ collisions at $\sqrt{s} = 1.96 \text{ TeV}$ recorded with the CDF II detector in Tevatron Run II. Modeling the resonance as a narrow massive vector boson Z' , and calculating its mass with techniques used in precision measurement of the top quark mass [11], we set limits on the cross section times branching ratio $\sigma B = \sigma(p\bar{p} \rightarrow Z') \cdot Br(Z' \rightarrow t\bar{t})$ as a function of $M_{Z'}$. This study is complementary to Ref. [12], which uses a different event selection and reconstruction of the $t\bar{t}$ kinematics.

The CDF II detector comprises a spectrometer in a 1.4 T magnetic field surrounded by projective electromagnetic and hadronic calorimeters and muon detectors [13]. The spectrometer, consisting of silicon microstrip detectors surrounded by a large open cell drift chamber, provides precision track reconstruction and displaced secondary vertex detection. We use coordinates where ϕ is the azimuthal angle, θ is the polar angle with respect to the proton beam axis, transverse energy is $E_T = E \sin(\theta)$, and the pseudorapidity is $\eta = -\ln[\tan(\theta/2)]$. The data used here were recorded between March 2002 and January 2006.

We collect a sample of $t\bar{t} \rightarrow W^+ b W^- \bar{b}$ candidate events with one leptonic W boson decay using triggers that require a central ($|\eta| \leq 1.0$) electron with $E_T > 18 \text{ GeV}$ or central muon with transverse momentum $p_T > 18 \text{ GeV}/c$. After offline reconstruction, we select events with an iso-

lated electron with $E_T \geq 20 \text{ GeV}$ or muon with $p_T \geq 20 \text{ GeV}/c$, missing transverse energy $\cancel{E}_T \geq 20 \text{ GeV}$ consistent with a neutrino from W decay, and at least four hadronic jets with $|\eta| \leq 2.0$, of which three must have $E_T \geq 15 \text{ GeV}$, and a fourth must have $E_T \geq 8 \text{ GeV}$ [14]. The jets are clustered in fixed cones of radius $\Delta R = \sqrt{(\Delta\eta)^2 + (\Delta\phi)^2} \leq 0.4$. At least one of the jets is required to be b -tagged, i.e. contain a reconstructed secondary vertex displaced from the primary event vertex as expected from the decay of a bottom hadron in the jet [15]. We find 347 events fulfilling these criteria.

The sample is dominated by s -channel $q\bar{q}$ annihilation into $t\bar{t}$ pairs [16,17]. The $t\bar{t}$ acceptance and efficiencies are calculated using the HERWIG generator [18] and a detector simulation, assuming a top mass $M_t = 175 \text{ GeV}/c^2$. The simulated detector response, particularly with respect to lepton isolation, jet energies, and b -tagging, has been tuned in an earlier measurement of the top pair production cross section [14]. The total combined trigger and reconstruction efficiency is $3.5 \pm 0.5\%$. Non- $t\bar{t}$ backgrounds include W bosons produced in association with jets ($W + \text{jets}$), where a light flavor jet is incorrectly b -tagged; $W + \text{jets}$ events with real heavy-flavor jets; mismeasured QCD multijet events with one jet identified as a lepton; and smaller contributions from electroweak processes such as diboson (WW , WZ , ZZ) and single-top production. The rates and kinematics of these processes are modeled with simulated and data control samples as employed in the top cross section measurement [14]. A total of 73 ± 9 non- $t\bar{t}$ background events are expected.

The final state of four jets, a high- p_T lepton, and \cancel{E}_T allows an over-constrained (2C) reconstruction of the top pair kinematics. The assignment of jets to quarks most consistent with the $t\bar{t}$ hypothesis is determined using the χ^2 minimization algorithm employed in the measurement of the top mass [11]. Here, following [19], we include the known top mass as a constraint, which improves the accuracy of the parton assignments. The measured jet energies are corrected back to parton values using calibrations derived from photon-jet balancing and detector simulation [20]. In the χ^2 minimization the parton energies are varied

LIMITS ON THE PRODUCTION OF NARROW $t\bar{t}$...

within their uncertainties and the W and top masses are constrained to the values $M_W = 80.4 \text{ GeV}/c^2$ and $M_t = 175.0 \text{ GeV}/c^2$ within their natural widths (2.1 and $1.5 \text{ GeV}/c^2$, respectively). The effect of variation in the central value of M_t is included later as a systematic uncertainty. Jets with b -tags must be associated with b quarks. The jet-quark assignment giving the lowest χ^2 consistent with these constraints is chosen as the solution. In simulated $t\bar{t}$ events we find a small number of poorly reconstructed events flagged by extreme χ^2 . We find the sensitivity of the search is optimized by requiring $\chi^2 < 50$; this cut removes 4% of $t\bar{t}$ events and 9% of non- $t\bar{t}$ backgrounds.

We model the resonant $t\bar{t}$ production mechanism as a sequential Z' , a heavy neutral boson with the same couplings as the Z , here including decay to $t\bar{t}$ with $M_{Z'} = 175 \text{ GeV}/c^2$. This color-singlet resonance has no interference with the standard color-octet $t\bar{t}$ production processes and the model lineshape is purely Lorentzian. To facilitate comparison to other results [9,10,12] we assign the same narrow width used there, $\Gamma_{Z'} = 0.012M_{Z'}$. A strictly sequential Z' with open $t\bar{t}$ decays has $\Gamma_{Z'} \approx 0.03M_{Z'}$. Since our reconstructed mass resolution is greater than $60 \text{ GeV}/c^2$ (see below) the analysis is insensitive to model dependent width differences at this level, and applies to any narrow $t\bar{t}$ state appearing as a single enhancement in the $M_{t\bar{t}}$ spectrum. Signal models are generated using the PYTHIA simulation [21] with Z' masses between 450 and 900 GeV/c^2 in increments of $50 \text{ GeV}/c^2$.

The inset of Fig. 1 shows the $M_{t\bar{t}}$ distribution reconstructed for a simulated $750 \text{ GeV}/c^2 Z'$. There is a peak near the expected value and a low mass tail which arises from the incorrect jet-parton assignments where a jet from initial or final state radiation has been used instead of a jet from top decay. The rms of the peak region is approximately $60 \text{ GeV}/c^2$ and the full rms is $137 \text{ GeV}/c^2$. Other Z' masses show similar behavior: the $M_{Z'}$ peak width is preserved and the low mass tail extends down to the kinematic threshold at $350 \text{ GeV}/c^2$. The full rms of the $M_{t\bar{t}}$ distribution varies between 67 and $178 \text{ GeV}/c^2$ over our Z' mass range. The fraction of Z' removed by the χ^2 cut varies between 4% and 9% over the Z' mass range.

We use a three-parameter binned likelihood maximization to fit the $M_{t\bar{t}}$ spectrum to a superposition of the expected shapes for $Z' \rightarrow t\bar{t}$, standard model $t\bar{t}$, and non- $t\bar{t}$ processes. In the i th bin, we expect

$$\mu_i = \left[\sigma B A \epsilon \int \mathcal{L} dt \right] P_{Z',i} + N_{t\bar{t}} P_{t\bar{t},i} + N_{\text{bkg}} P_{\text{bkg},i} \quad (1)$$

where $P_{Z',i}$, $P_{t\bar{t},i}$, and $P_{\text{bkg},i}$ are the probabilities of observing a signal event, $t\bar{t}$ event or non- $t\bar{t}$ background event in bin i , respectively. $N_{t\bar{t}}$ and N_{bkg} are the number of non-resonant $t\bar{t}$ and the non- $t\bar{t}$ background events. The $\sigma B A \epsilon \int \mathcal{L} dt$ term contains the product of cross section

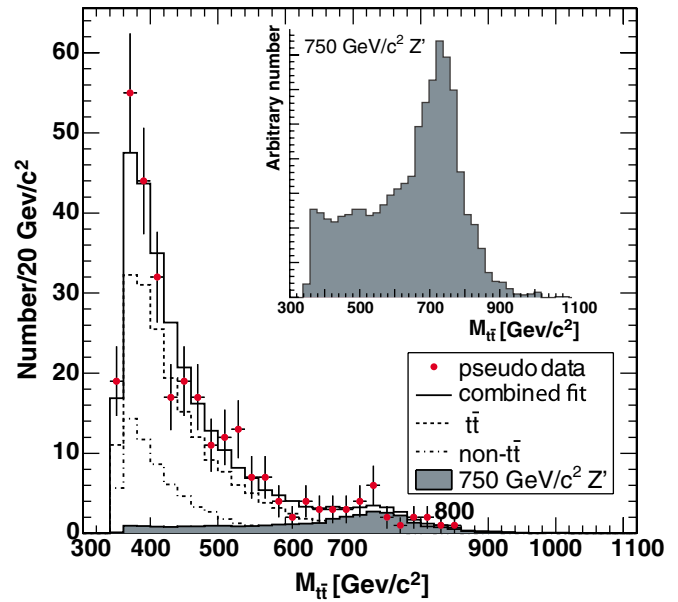


FIG. 1 (color online). Simulated $M_{t\bar{t}}$ spectrum for 955 pb^{-1} in presence of a $750 \text{ GeV}/c^2 Z'$ with $\sigma B = 1 \text{ pb}$ (shaded curve). The points are a simulated data set. The solid line is the best fit to a superposition of the Z' signal (solid histogram) and the expected $t\bar{t}$ (dot line) and non- $t\bar{t}$ (dot-dash line) backgrounds. The inset shows the reconstructed $M_{t\bar{t}}$ spectrum in an arbitrarily large sample of simulated $750 \text{ GeV}/c^2 Z'$. The low mass tail arises from incorrect jet-parton associations.

and $t\bar{t}$ branching ratio, acceptance, and efficiency for the Z' , and the luminosity.

A likelihood function L for the distribution can be written as

$$L = \prod_{i,k} \mathcal{P}_i(n_i | \mu_i) G(\nu_k | \bar{\nu}_k, \sigma_{\nu_k}). \quad (2)$$

The function $\mathcal{P}_i(n_i | \mu_i)$ is the Poisson probability for observing n_i events in a bin i where μ_i are expected. The functions $G(\nu_k | \bar{\nu}_k, \sigma_{\nu_k})$ constrain the nuisance parameters ν_k , which include the non- $t\bar{t}$ background normalization N_{bkg} , b -tag efficiency, acceptances and luminosities, with Gaussian probability around their central values $\bar{\nu}_k$ and uncertainties σ_{ν_k} . The $t\bar{t}$ and non- $t\bar{t}$ background values are taken from [14], and the Z' acceptances and efficiencies are determined from the PYTHIA simulation. We find σB , $N_{t\bar{t}}$, N_{bkg} , and ν_k that maximize the likelihood function for each $M_{Z'}$.

The algorithm is tested with simulated samples where the $t\bar{t}$, non- $t\bar{t}$, and Z' models are combined in the expected ratios and sampled with the expected level of statistical fluctuations. The points in the main part of Fig. 1 show the $M_{t\bar{t}}$ distribution for a simulated data sample corresponding to an integrated luminosity of 955 pb^{-1} in the case of a $750 \text{ GeV}/c^2 Z'$ with $\sigma B = 1 \text{ pb}$. The histograms show the components as resolved by the likelihood fit. The extrac-

tion of the Z' component uses shape information from the low mass part of the spectrum as well as the peak area.

The 95% C.L. upper limit on σB at a given mass is found by integrating the likelihood along σB , reoptimizing at each point, to find the value that contains 95% of the area. We measure our expected sensitivity using large ensembles of simulated samples like the one shown in Fig. 1. The main sources of systematic uncertainty are the acceptance change due to energy scale uncertainty on the jet thresholds, and the shape change in $M_{t\bar{t}}$ from the top mass uncertainty of 3 GeV/ c^2 . Model dependent shape effects associated with initial and final state gluon radiation and non- $t\bar{t}$ backgrounds are small. PDF uncertainties are evaluated using simulated samples generated with MRST [22] and the full set of eigenvectors from CTEQ6M [23]. Simulated samples with reasonable variations for systematic effects are used to measure the apparent shifts in the fitted σB as a function of the true value. The sum of the shifts in quadrature is used as the width of a Gaussian resolution function that is convolved with the likelihood as a function of σB . The systematic uncertainties worsen the limits by roughly 0.2 pb, independent of the Z' mass, with the increase dominated by the effects of jet energy scale and the top mass uncertainty in equal measure. The expected 95% C.L. upper limits including all sources of uncertainty are shown as a function of $M_{Z'}$ in the middle column of Table I. If no Z' is present our expected cross section limit at high $M_{Z'}$ is 0.55 pb.

The $M_{t\bar{t}}$ distribution measured in the data is shown in Fig. 2. A final sample of 327 candidates remains after the χ^2 requirement. In this figure we compare the observation to the expected spectrum in the case of no Z' . The non- $t\bar{t}$ component is fixed at the expected value and the $t\bar{t}$ normalization is scaled to match the total number of events. The inferred top production cross section is $\sigma(t\bar{t}) = 7.8 \pm 0.7$ pb (statistical error only), to be compared with the predicted standard model value of 6.7 pb for $M_t = 175$ GeV/ c^2 [16,17]. The inset shows the measurement

TABLE I. Expected and observed limits (95% C.L.) on $\sigma(p\bar{p} \rightarrow Z') \cdot Br(Z' \rightarrow t\bar{t})$ as a function of $M_{Z'}$ for 955 pb $^{-1}$, including both statistical and systematic uncertainties.

$M_{Z'}(\text{GeV}/c^2)$	Expected Limit (pb)	Observed Limit (pb)
450	$2.27^{+0.79}_{-0.57}$	3.39
500	$1.92^{+0.63}_{-0.40}$	2.72
550	$1.37^{+0.45}_{-0.30}$	1.57
600	$0.97^{+0.33}_{-0.18}$	0.83
650	$0.78^{+0.24}_{-0.13}$	0.65
700	$0.70^{+0.14}_{-0.12}$	0.64
750	$0.64^{+0.15}_{-0.11}$	0.61
800	$0.58^{+0.15}_{-0.07}$	0.60
850	$0.55^{+0.10}_{-0.05}$	0.57
900	$0.55^{+0.08}_{-0.06}$	0.57

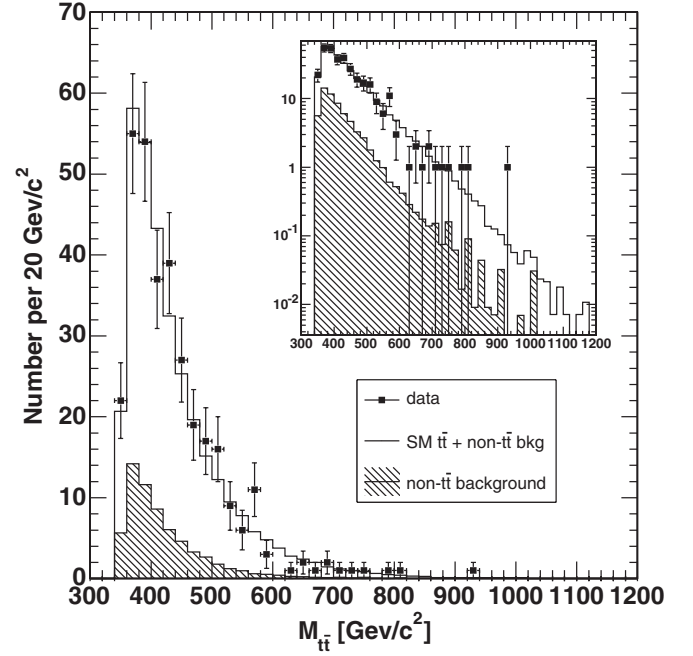


FIG. 2. The invariant mass of top quark pairs $M_{t\bar{t}}$ observed in the data is compared to the no Z' expectation. The non- $t\bar{t}$ backgrounds are constrained to the expected value and the sum of $t\bar{t}$ and non- $t\bar{t}$ equal the number of data events.

on a logarithmic scale. The simulated $M_{t\bar{t}}$ spectra for $t\bar{t}$ and non- $t\bar{t}$ describe the data well.

Applying the full limit procedure to the spectrum in Fig. 2 we find 95% C.L. upper limits on $\sigma(p\bar{p} \rightarrow Z') \cdot Br(Z' \rightarrow t\bar{t})$ as listed in the rightmost column of Table I. The limits at high mass are consistent with expectation. At lower masses our measurement shows an excursion above the expected value of approximately 1 standard deviation.

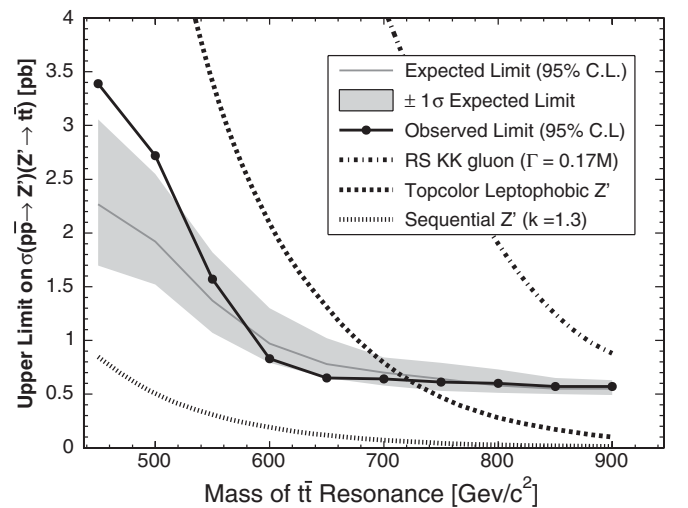


FIG. 3. Upper limits (95% C.L.) on the production cross section for $t\bar{t}$ resonance along with expected cross sections for several models.

The result is represented graphically and compared to some theoretical predictions in Fig. 3. The observed limit is the solid black line and the shaded band around the gray line denotes the $\pm 1\sigma$ uncertainties around the expected upper limit. A leptophobic Z' predicted by the top color theory [4], shown as a large-dotted line, is ruled out below $720 \text{ GeV}/c^2$ at 95% C.L. The small-dotted curve at the bottom of the figure is the expected cross section for a sequential Z' , calculated with the HERWIG simulation using a multiplicative factor of 1.3 to account for NLO effects. A leptophobic Z' with these couplings would evade direct searches in dilepton final states, and because the $t\bar{t}$ detection efficiency is small, is still out of range of our sensitivity in the $t\bar{t}$ mode. The Tevatron cross section for the KK gluon excitation in the Randall-Sundrum model of Ref. [6] is shown as a dot-dash line [24]. Since the KK resonance is broad ($\Gamma \approx 0.17M$), our limits derived in the “narrow width” assumption are not strictly applicable; we show the curve here for qualitative comparison. The cross section of any narrow Z' -like state produced in $p\bar{p}$ collisions at $\sqrt{s} = 1.96 \text{ TeV}$ and subsequently decaying to $t\bar{t}$ is less than or equal to 0.64 pb (95% C.L.) for all $M_{Z'}$ above $600 \text{ GeV}/c^2$.

We thank the Fermilab staff and the technical staffs of the participating institutions for their vital contributions. This work was supported by the U.S. Department of Energy and National Science Foundation; the Italian Istituto Nazionale di Fisica Nucleare; the Ministry of Education, Culture, Sports, Science and Technology of Japan; the Natural Sciences and Engineering Research Council of Canada; the National Science Council of the Republic of China; the Swiss National Science Foundation; the A.P. Sloan Foundation; the Bundesministerium für Bildung und Forschung, Germany; the Korean Science and Engineering Foundation and the Korean Research Foundation; the Science and Technology Facilities Council and the Royal Society, UK; the Institut National de Physique Nucleaire et Physique des Particules/CNRS; the Russian Foundation for Basic Research; the Comisión Interministerial de Ciencia y Tecnología, Spain; the European Community’s Human Potential Programme; the Slovak Research and Development Agency; and the Academy of Finland.

-
- [1] J. Rosner, Phys. Lett. B **387**, 113 (1996).
 - [2] A. Leike, Phys. Rep. **317**, 143 (1999).
 - [3] M. Carena, A. Daleo, B. A. Dobrescu, and T. M. P. Tait, Phys. Rev. D **70**, 093009 (2004).
 - [4] C. Hill and S. Parke, Phys. Rev. D **49**, 4454 (1994).
 - [5] L. Sehgal and M. Wanninger, Phys. Lett. B **200**, 211 (1988).
 - [6] B. Lillie, L. Randall, and L. T. Wang, J. High Energy Phys. **09** (2007) 074.
 - [7] G. Burdman, B. Dobrescu, and E. Ponton, Phys. Rev. D **74**, 075008 (2006).
 - [8] L. Fitzpatrick, J. Kaplan, L. Randall, and L. T. Wang, J. High Energy Phys. **09** (2007) 013.
 - [9] A. Affolder *et al.* (CDF Collaboration), Phys. Rev. Lett. **85**, 2062 (2000).
 - [10] V. Abazov *et al.* (D0 Collaboration), Phys. Rev. Lett. **92**, 221801 (2004).
 - [11] A. Abulencia *et al.* (CDF Collaboration), Phys. Rev. D **73**, 032003 (2006).
 - [12] T. Aaltonen *et al.* (CDF Collaboration), arXiv:0709.0705 [Phys. Rev. Lett. (to be published)].
 - [13] D. Acosta *et al.* (CDF Collaboration), Phys. Rev. D **71**, 032001 (2005).
 - [14] A. Abulencia *et al.* (CDF Collaboration), Phys. Rev. Lett. **97**, 082004 (2006).
 - [15] D. Acosta *et al.* (CDF Collaboration), Phys. Rev. D **71**, 052003 (2005).
 - [16] N. Kidonakis and R. Vogt, Phys. Rev. D **68**, 114014 (2003).
 - [17] M. Cacciari, S. Frixione, G. Ridolfi, M. Mangano, and P. Nason, J. High Energy Phys. **04** (2001) 068.
 - [18] G. Corcella *et al.*, J. High Energy Phys. **01** (2001) 010.
 - [19] A. Abulencia *et al.* (CDF Collaboration), Phys. Rev. D **73**, 111103 (2006).
 - [20] A. Bhatti *et al.*, Nucl. Instrum. Methods Phys. Res., Sect. A **566**, 375 (2006).
 - [21] T. Sjostrand *et al.*, Comput. Phys. Commun. **135**, 238 (2001).
 - [22] A. D. Martin, R. G. Roberts, W. J. Stirling, and R. S. Thorne, Eur. Phys. J. C **14**, 133 (2002).
 - [23] J. Pumplin, Nucl. Instrum. Methods Phys. Res., Sect. A **447**, 1 (2002).
 - [24] The Tevatron curves were generated by Ben Lillie, based on work in Ref. [6].